

GOCE GRADIENT TENSOR CHARACTERIZATION OF THE COUPLED PARANÁ (SOUTH AMERICA) AND ETENDEKA (AFRICA) MAGMATIC PROVINCES

Patrizia Mariani⁽¹⁾, Carla Braitenberg⁽²⁾

Department of Mathematics and Earth Sciences, University of Trieste, Italy

⁽¹⁾ Email: pmariani@units.it

⁽²⁾ Email: berg@units.it

ABSTRACT

The Paraná-Etendeka Large Igneous Province (LIP) at the conjugate plate margins of South America and Africa is investigated with GOCE gradients. The LIP is associated to Gondwana breakup, and is asymmetric between the two margins. The study intends to investigate how the lithosphere is affected by continental breakup and what caused the asymmetry, considering that successive spreading is symmetric. The gradients at satellite and surface height are modelled with other geophysical data as seismic profiling, seismic tomography and bore-hole logs. Densities and velocities are modelled with a petrologic model. The residual gravity gradients, reduced of crustal thickness variations and sediments, are continuously high along the Angola and Namibia margin. Inversion shows the high is due to a density increase about 6 km thick with the top at about 23 km depth, placing it above the Moho. It is probable that the densification be due to magmatic intrusions, increasing the volume of the LIP at the African side, which remained trapped in the crust and produced only small volumes of surface basalts. This is true also for the margin of Angola, which in literature is claimed to be void of magmatism along its margin.

1. INTRODUCTION

The Paraná-Etendeka Large Igneous Province (LIP) straddles the two continents South-America (SAM) and Africa in the countries of Brazil and Angola-Namibia. The LIP is 135 Ma [1] and is associated to the breakup of Western Gondwana [2]. The areal extension of the basalts on the Brazilian side is much larger than on the African side [3] indicating an asymmetry in the volcanism producing the LIP. The reason for the asymmetry could reside in the position of the magmatic source, which should be closer to the Brazilian side and only marginally affect the African plate. Otherwise it could be explained by a position below the future margin, but with a less permeable lithosphere on the African side, that blocked the effusion of the magmatic products to the surface [4]. The study uses the newest GOCE products to better understand the lithosphere of the now separated, once united Paraná-Etendeka magmatic provinces. Of interest are the unknown masses below the basins, crustal thickness, and

subcrustal density alterations due to the magmatism of the LIP.

The contributions of sediments, crustal thickness and mantle density variations to the gradient are forward modelled resulting in the residual gradient tensor. The calculation of the gradient field is made with the release 5 of the TIM gravity potential model and considering two different heights: 10 and 250 km.

The calculations are performed for South America centred on the Paraná intracratonic basin, and for Western Africa including the Etendeka region, e.g. Angola and Namibia.

The layered forward model allows to characterize the different contributions to the tensor field at 10 km and at satellite height (250 km), which is useful for a better understanding of the sensitivity of the tensor components. The Angola-Namibia margin has been claimed to change from a volcanic passive continental margin to non-volcanic margin going from Namibia [5], [6] to Angola [7], [8]. The gradient residual fields result in a continuous gravity high along the margin, that suggests densification along the entire margin. A compatible model would be a increased density above the Moho several km thick, which could be due to trapped magmatic intrusions that did not reach the surface to outpour magmatic products.

2. GEOPHYSICAL DATA

The gravity gradients are calculated through spherical harmonic synthesis up to degree and order 250 from the global gravity model GO_CONS_GCF_2_TIM_R5, produced by the Graz University of Technology, Institute for Theoretical and Satellite Geodesy, University of Bonn, Institute of Geodesy and Geoinformation and TU München, Institute of Astronomical and Physical Geodesy [9]. The gradients are calculated at a height of 10 km and 250 km above a sphere of radius 6.3781363e+06 m using the software Manipulator [10]. The T_{rr} component is shown in Fig. 1 for the African and Brazilian margins. The crustal layers are subdivided from top to bottom between the topography, sediments and the crust-mantle boundary, overlying the mantle. The topography model is ETOPO1 [11] with resolution of 1 arcmin.

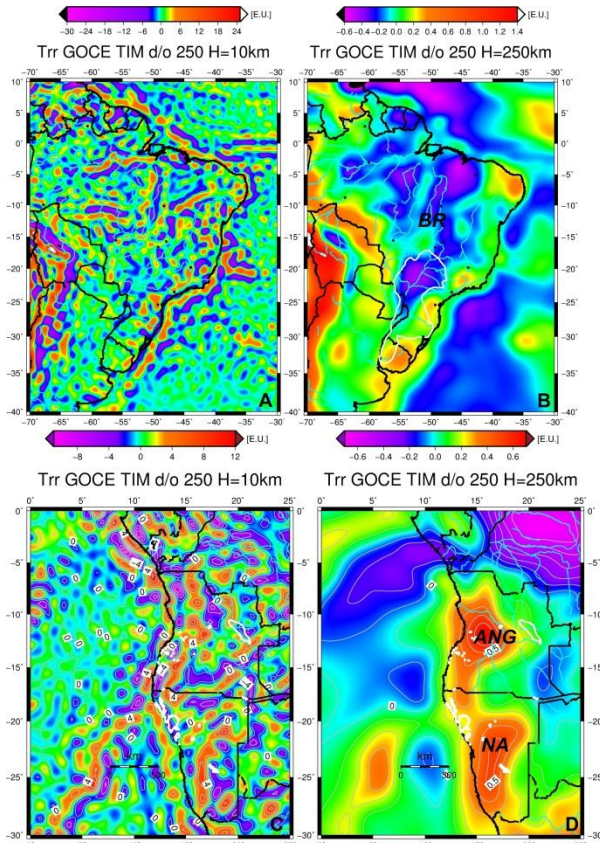


Figure 1. Trr in South America and Africa studied area at 10 and 250 km (the label are: BR Brazil, ANG Angola, and NA Namibia).

The global tomographic model LLNL-G3Dv3 [12] has V_p velocities at a 1° grid resolution in the upper mantle. Sedimentary rock isopachs are taken from the PLATES project onshore [13] and from National Geophysical Data Center (NGDC), NOAA offshore [14]. A high quality Moho depth model for South America is available on a 0.5° resolution grid [15]. For the volcanic Paraná province a detailed database of the pre-volcanic, volcanic and post-volcanic isopach layers [16] was used to integrate the global sediment model. On the African side the sedimentary rocks isopachs are available from the publication [17] onshore. The Moho in Africa is more problematic and less well constrained. The solution of [18] combines gravity and seismologic observations, and is thus not independent from gravity data. The CRUST1.0 model [19] has filled-in zones obtained from geological analogies where measurements were unavailable and thus is only partly reliable. Here an isostatic Moho has been calculated for comparison. A cartoon showing the different layers is shown in Fig. 2.

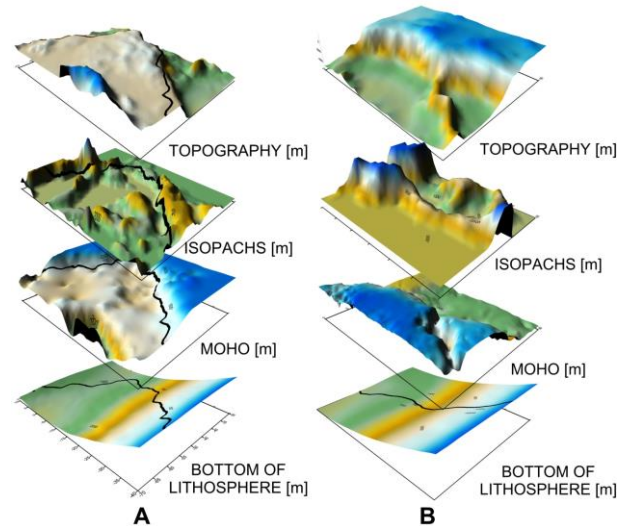


Figure 2. Cartoon with main database layers: topography, sediment isopachs, Moho and base lithosphere in South America (A) and Africa (B).

3. FORWARD MODELING RESULTS

3.1. Crustal layers

The database of the crustal layers was used to forward model the gravity gradients using a discretization with tesseroids [20]. Given the geometries, some uncertainties exist on the densities. For sediments density is taken to increase with depth and with age. At the crust-mantle boundary a range of plausible density contrasts and depths for the reference crustal model was tested, allowing a range from 30 to 35 km for the reference depth, and a density range between 300 and 500 kg/m^3 . The preferred values are reference depth 35 km for Paraná and 30 km for Etendeka, with density contrast respectively 500 and 400 kg/m^3 . Tab. 1 gives the range, average and standard deviation of the calculated gradient values for the sedimentary rocks and Moho using the preferred parameters over the studied areas defined by coordinates 35° and 65°W , 35°S and 5°N for South America and 5° and 20°E and 5° and 25°S for Africa, respectively. The contributions of sediments on the South American side is greater than on the African side, due to the post-volcanic thick sediments of the Paraná basin. For Etendeka the preferred model is the Commission for the Geological Map of the World CGMW/Unesco model [17], which differs considerably from the PLATES [13] model onshore. The maximum Trr signal without any correction at 10 and 250 km on the South American side is respectively around ± 50 and ± 1.5 Eötvös, smaller values occur in Etendeka. After the topographic correction the tensor is positive off-shore due to the Moho shallowing. At 10 km height, the effect of the basins is small (2-5 E.U.) with respect to those of the crustal root (± 10 E.U.). In general at 250 km calculation height the signal is very small (around ± 0.5 E.U.); only

the crustal thickening effect is more than 2 E.U; the signal of the small basins is very wide in wavelength but recognizable. In Tab. 1 the extreme value of T_{rr} (Min, Max) with the Mean (M) and Standard Deviation (STD) for the separate contribution of Moho and sedimentary rocks are shown. The table gives calculation height (H), reference depth (D), and density (d) for Moho. In SAM the Moho is from reference [15] and the isostatic model, in Etendeka for the reference [18]. For the Paraná, the layers are: the pre-volcanic layer, the volcanic layer, and the post-volcanic layer onshore, and a unique layer offshore [14]. For Etendeka the CGMW/Unesco [17], Plates [13] and NOAA model [14] are compared. A detailed discussion for the layers in Paraná are found in [16].

MOHO	H	D	d	Min	Max	M	STD
PARANÁ	10	35	500	-11.4	11.3	0.2	3.5
	10	35	500	-19.7	20.9	0.3	5.0
	250	35	500	-3.6	3.8	0.2	1.4
	250	35	500	-6.0	5.4	0.3	2.4
ETENDEKA	10	30	400	-10.4	11.7	0.5	5.2
	10	30	400	-8.1	11.5	0.9	5.4
	250	30	400	-2.5	4.3	0.6	2.4
	250	30	400	2.4	4.9	0.7	2.5

A

SED	H	isopachs	Min	Max	M	STD
PARANÁ	10	Pre-volc	-6.07	3.90	-0.04	0.57
		Volc	-0.88	1.18	0.0	0.10
		Post-volc	-14.2	5.88	0.0	0.70
		NOAA	-17.3	8.85	-0.04	1.66
	250	Pre-volc	-0.27	0.05	0.03	0.07
		Volc	0.0	1.12	0.0	0.01
		Post-volc	-0.42	0.02	0.0	0.04
		NOAA	-0.92	0.10	0.05	0.18
ETENDEKA	10	CGMW/Unesco	-1.36	0.68	0.0	0.08
		Plates	-7.7	5.26	-0.38	2.03
		NOAA	-11.0	9.52	0.03	1.7
	250	CGMW/Unesco	-0.92	0.10	0.05	0.18
		Plates	-0.19	0.01	0.0	0.02
		NOAA	-1.20	0.16	-0.19	0.34

B

Table 1. Statistical values of T_{rr} effect for Paraná and Etendeka. H is the height of calculation, M average, STD standard deviation. A: Moho effect: seismological model (bold) Assumpção model [15] in SAM, and Tugume model [18] in Etendeka. Normal text for isostatic Moho. D is the reference depth in km, d is the contrast density in kg/m^3 . B: the T_{rr} of Sedimentary rocks using different models for the layer isopachs in SAM and Etendeka.

3.2. Mantle layers

The modelling of the density variations in the mantle must consider the petrological composition of the mantle and the temperature and pressure conditions with depth. Information on mantle composition is retrieved from geophysical studies, mantle xenolites and ophiolites, which are made of uplifted oceanic crust and upper mantle. Reference [21] defined standard petrological classification of lithosphere with the percentages of four lead minerals: Olivine, Orthopyroxene, Clinopyroxene and Garnet. The percentages are defined according to lithosphere age in Archean, Proterozoic and Phanerozoic, each having a different proportion in the lead minerals. The seismic velocity and density for the lead minerals in function of temperature and pressure has been defined by [22]. The method includes the physical laws governing density and seismic velocity in function of temperature and pressure combined with laboratory measurements of a great number of mineral samples. Given the percentages of the lead minerals, the bulk density and velocity are also calculated. There are uncertainties on the temperature and pressure gradient for our two conjugate margins, so plausible values are tested. The temperature at base lithosphere is kept constant ($1300^{\circ}C$), varying the temperature at base Moho according to the age of the most recent tectonic event between 400° and 1000° . The predicted velocities are compared to the observed velocities of the tomographic model [12] to verify the model. Fig. 3 shows the V_p profile for selected regions with the modelled V_p from the mineralogical model. The agreement is very good, with the predicted velocities following the observed velocities well. Assuming that a correct reproduction of the velocities is a verification of the assumed petrological model, the predicted densities are used for modelling the mantle contribution down to 300 km to the gravity gradients. The model predicts an increase of density with depth, amounting to a relative increase from Moho to bottom of lithosphere of $120 kg/m^3$. The increase is greater for the Proterozoic mantle compared to the Phanerozoic mantle. The temperature effect corresponds to a density decrease for increasing temperature. Increase in pressure leads to a higher density. In the lithosphere the increase in density due to the pressure increase prevails over the density reduction due to the temperature increase. With constant pressure conditions, a higher temperature at the Moho will lead to a lower density below Moho and to an average lower density down until it reaches base lithosphere. Presently the modelling of the mantle densities is in the testing stage, and further developments are necessary for the complete reduction of the gradients. The mantle effect for our study area is in the order of 2 E.U. for T_{rr} at the height of 10 km, and in the order of 0.4 E.U. at the height of 250 km.

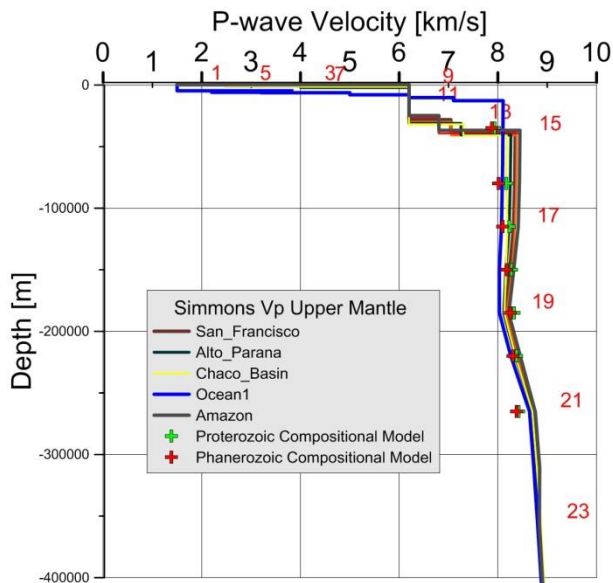


Figure 3. P-wave velocity according to LLNL_G3Dv3 tomographic model [12]. Crosses are velocities from petrologic model described in text.

3.3. Description of the Trr residual field

The residual gradient for the Paraná-Etendeka regions is shown in Fig. 4 for Trr at the heights of 10 km and 250 km, respectively. The Trr signal, the most straightforward to understand, is centered on the mass anomaly, but also can have an opposite signal marking the border. This shape is like a dipole. For instance a pronounced negative signal over a sedimentary basin has low amplitude and positive tails at the edge. Viceversa an increased density gives the opposite pattern. It is interesting to see that for some basins a positive residual Trr signal is seen both at 10 km and 250 km height, as over the Paraná region and also along the Brazilian and Etendeka shore line, in relationship with the off-shore volcanic province. Obviously the signal is more defined at the lower height.

At 250 km broad scale variations prevail, some of which are also found in the 10 km residual. Those anomalies which are consistent at both heights presumably affect the entire lithosphere from deep to shallow layers. The short scale anomalies only found at 10 km height presumably are generated by shallower density variations limited to the crust. Over the Amazon basin for instance a broad high is found, that has no correlation to the pattern found at 10 km height. The high over the Paraná basin, over the Parnaíba and the low south of the Amazon are coherent patterns at 250 km and 10 km height. On the African side along the entire margin a continuous high is found, which is coherent both at 10 km and 250 km height. This continuous high is not found on the Brazilian side, where it is limited to latitudes -31° to -24° . In the next step a forward modelling is accomplished to test at

which depth the source could be located that generates the linear high along the African margin.

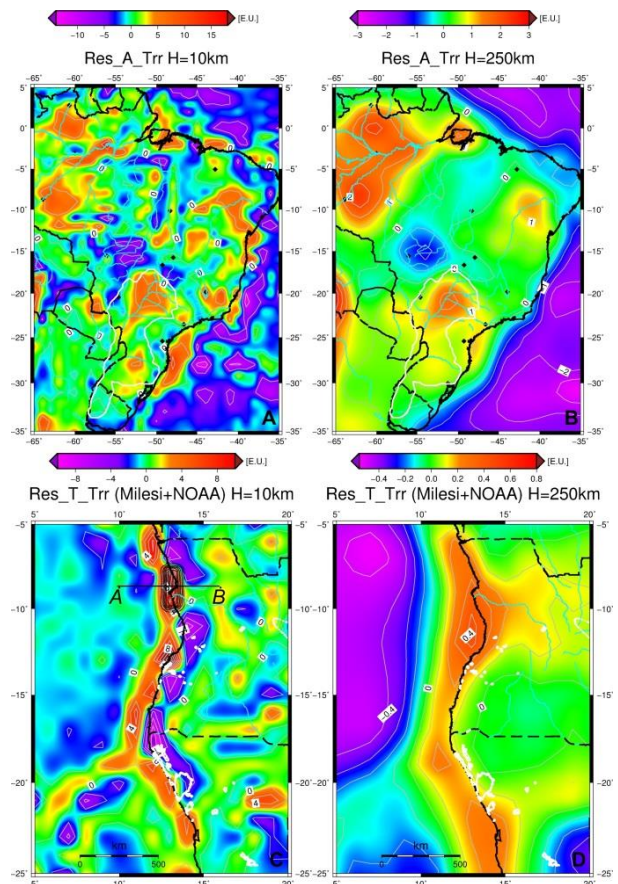


Figure 4. Residual vertical gradient on conjugate Paraná-Etendeka margins at 10 and 250 km height. In A and B the residual Trr of Paraná at 10 and 250 km, in C and D the Etendeka at 10 and 250 km. In C: profile of forward model.

4. RESIDUAL MODELING

The problem consists in estimating the depth and size of the source that generates the linear Trr high along the Angola and Namibia margin. Presently the inversion algorithm for the full set of gradients is under development, so a forward model must be done. Seismic investigation studies crossing the margin are available, constraining the superficial part of the margin. The active seismic gives no evidence for superficial magmatic intrusions, which sets the source of the positive anomaly in the lower crust or in the upper mantle. A source in the upper crust would be explainable by magmatic intrusions along the margin that accompanied the LIP but did not reach the surface. The modelled and observed curves of a section parallel to the available seismic lines is shown in Fig. 5. The source is a prism 1° wide, 2.5° long, 6 km thick, placed above the Moho (bottom at 29 km depth), with a density contrast of 250 kg/m^3 . This model is a first

approximation of one solution to the source of the anomaly.

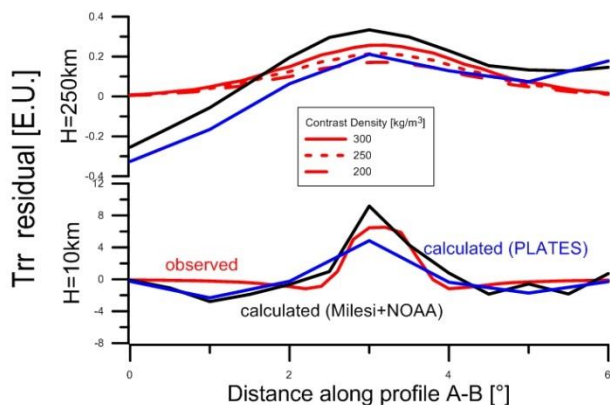


Figure 5. Modeling of T_{rr} residual, with crustal intrusion, details in text. Profile A-B located in Fig. 4 C.

5. DISCUSSION

The gradient field derived from the GOCE only model for the conjugate margins of the Paraná-Etendeka LIP bear signals that are useful for understanding the lithosphere evolution which has undergone Western Gondwana breakup. In a previous study the Paraná basin and the igneous province was studied in detail integrating gravity and seismologic data [16]. Main result was the recognition of a discrepancy between the very deep Moho recovered from seismological studies (48 km) and the observed gravity field. The observations were not explainable with a homogeneous lower crust, and required the presence of underplating below the Paraná basin. Petrologically this material with increased density was explained by Gabbro, which was trapped in the lower crust and was the densified magma which released the lighter basalt forming the LIP present in the successions of the Paraná basin. The LIP extends to the African margin, but the basalts extend over a much smaller area limited along the coast and lacking the extension of the Paraná basin. The residual T_{rr} positive linear field along the African margin seems to be also due to a densified lower crust, as the observations could be explained with such a source. The LIP would therefore have very different geometries on the South American and African side, but have in common the densified lower crust, which could in both cases be due to magmatic underplating.

6. CONCLUSIONS

Here it is demonstrated that the analysis of the gradients observed by GOCE is a useful tool to identify the relationship between the Angola-Namibia and Brazilian margins straddled by the Paraná-Etendeka LIP. It is found that along both margins large magmatic masses are trapped in the crust tied to the LIP. A portion of the

underplating could also be due to the magmatic processes that accompanied the South Atlantic Ocean opening.

7. ACKNOWLEDGEMENTS

PM is partially supported under a programme of and funded by the European Space Agency, scientific resp. CB. The view expressed herein can in no way be taken to reflect the official opinion of the European Space Agency. We acknowledge use of the Generic Mapping Tools [23].

8. References

1. Thiede D.S. & Vasconcelos, P.M. (2010). Paraná flood basalts: Rapid extrusion hypothesis confirmed by new results $^{40}\text{Ar}/^{39}\text{Ar}$. *Geology Society of America*, **38**, 747-750, doi: 10.1130/G30919.1.
2. Emery, K.O., Uchupi, E., Phillips, J., Bowin, C. & Mascle, J. (1975). Continental margin off Western Africa: Angola to Sierra Leone, *Am. Assoc. Petrol. Geol. Bull.* **59**, 2202–2265
3. Uenzelmann-Neben, G. (2013). Magma Giant, *Nat. Geosc.* **6**, 202-203.
4. Becker K., Franke, D., Trumbull, R., Schnabel, M., Heyde, I., Schreckenberger, B., Koopmann, H., Bauer, K., Jokat, W. & Krawczyk, C.M. (2014). Asymmetry of high-velocity lower crust on the South Atlantic rifted margins and implications for the interplay of magmatism and tectonics in continental breakup. *Solid Earth*, **5**, 1011–1026.
5. Gladchenko, T.P., Skogseid J. & Eldhom, O. (1998). Namibia Volcanic Margin. *Mar. Geophys. Res.* **20**, 313–341.
6. Bauer, K., Neben, S., Schreckenber, B., Emmerman, R. Hinz, K., Fechner, N., Gohl, K., Schulzei, A., Trumbull, R.B. & Weber, K. (2000). Deep structure of the Namibia continental margin as derived from integrated geophysical studies. *J. Geophys. Res.* **105**(B11), 25829-25853.
7. Contrucci, I., Matias L., Moulin, M., Géli L., Klingelhofer F., Nouzé H., Aslanian D., Olivet J-L, Réhault J-P. & Sibuet, J-C. (2004). Deep structure of the West African continental margin (Congo, Zaïre, Angola), between 5°S and 8°S, from reflection/refraction seismics and gravity data. *Geophys. J. Int.* **158**, 529–553.
8. Moulin, M., Aslanian, D., Olivet J.L., Contrucci I., Matias L., Géli L., Klingelhofer F., Nouzé H., Réhault J-P. & Unternehr, P. (2005). Geological constraints on the evolution of the Angolan margin

- based on reflection and refraction seismic data (Za'Ango project). *Geophys. J. Int.* **162**, 793–810.
9. Pail, R., Bruinsma, S.L., Migliacchio, F., Foerste, C., Goiginger, H., Schuh, W.D., Hoeck, E., Reguzzoni, M., Brockmann, J.M., Abrikosov, O., Veicherts, M., Fecher, T., Mayrhofer, R., Krasbutter, I., Sansò, F. & Tscherning, C.C. (2011). First GOCE gravity field models derived by three different approaches. *J. Geod.* **85**, 819–843, doi: 10.1007/s00190-011-0467-x.
 10. Gatti, A. (2013). Spherical Harmonic Manipulator, <http://sourceforge.net/projects/hmanipulator/files/>
 11. Amante, C.B. & Eakins, W. (2008). ETOPO1 1 Arc-Minute Global Relief Model: Procedures, Data Sources and Analysis. National Geophysical Data Center, NESDIS, NOAA, U.S. Department of Commerce, Boulder, CO, August 2008.
 12. Simmons, N.A., Myers, S.C., Johannesson, G., & Matzel, E. (2012). LLNL-G3Dv3: Global P wave tomography model for improved regional and teleseismic travel time prediction. *J. Geophys. Res.* **117**, B10302, doi:10.1029/2012JB009525.
 13. Coffin, M.F., Gahagan, L.M., & Lawver, L.A. (1998). Present-day Plate Boundary Digital Data Compilation. University of Texas Institute for Geophysics, *Technical Report*, **174**, pp. 5.
 14. Divins, D.L. (2003). Total Sediment Thickness of the World's Oceans & Marginal Seas, NOAA National Geophysical Data Center, Boulder, CO.
 15. Assumpção, M., Feng, M., Tassara, A., & Juliá, J. (2013). Models of crustal thickness for South America from seismic refraction, receiver functions and surface wave tomography. *Tectonophysics*, **609**, 82–96, doi: 10.1016/j.tecto.2012.11.014.
 16. Mariani, P., Braitenberg, C. & Ussami, N. (2013). Explaining the thick crust in Paraná basin, Brazil, with satellite GOCE gravity observations. *J. South. Am. Earth Sc.* **45**, 209–223.
 17. Milesi, J.P., Frizon de Lamotte, D., de Kock, G. & Toteu, F. (2012). Tectonic Map of Africa (2nd edition). CGMW and Unesco (CD-room).
 18. Tugume, F., Nyblade, A., Juliá, J. & van der Meijde, M. (2013). Precambrian crustal structure in Africa and Arabia: Evidence lacking for secular variation, *Tectonophysics*, **609**, 250–266.
 19. Laske, G., Masters, G., Ma, Z., & Pasyanos, M. (2013). Update on CRUST1.0- A 1-degree Global Model of Earth's Crust, *Geophys. Res. Abstract* EGU2013.2658.
 20. Uieda, L. (2013). Tesseroids: Forward modeling of gravitational fields in spherical coordinates, figshare, <http://dx.doi.org/10.6084/m9.figshare.786514>, doi:10.6084/m9.figshare.786514.
 21. Artemieva, I.M. (2009). The continental lithosphere: Reconciling thermal, seismic, and petrologic data. *Lithos.* **109**, 23–46.
 22. Hacker, B.R. & Abers, G.A. (2004). Subduction Factory 3: An Excel worksheet and macro for calculating the densities, seismic wave speeds, and H₂O contents of minerals and rocks at pressure and temperature. *Geochem. Geophys. Geosystems*, **5**(1), Q01005, doi:10.1029/2003GC000614.
 23. Wessel, P., Smith, W.H.F., Scharroo, R., Luis, J.F. & Wobbe, F. (2013). Generic Mapping Tools: Improved version released, *EOS Trans. AGU*, **94**, 409–410.